IEEE Access
Multidisciplinary | Rapid Review | Open Access Journal

Received August 26, 2020, accepted September 8, 2020, date of publication September 10, 2020,
date of current version September 24, 2020.

Digital Object Identifier 10.1109/ACCESS.2020.3023275

NOMA-Based 802.11n for Industrial Automation

JON MONTALBAN[1], (Member, IEEE), ENEKO IRADIER[1], (Graduate Student Member, IEEE), PABLO ANGUEIRA[1], (Senior Member, IEEE), OSCAR SEIJO[2], (Member, IEEE), AND IÑAKI VAL[2], (Senior Member, IEEE)

[1]Department of Communications Engineering, University of the Basque Country (UPV/EHU), 48013 Bilbao, Spain
[2]IKERLAN Technology Research Centre, Basque Research and Technology Alliance (BRTA), 20500 Mondragón, Spain

Corresponding author: Eneko Iradier (eneko.iradier@ehu.eus)

This work was supported in part by the Basque Government under Grant IT1234-19, in part by the PREDOC Grant Program under Grant PRE_2019_2_0037 and project U4INDUSTRY (ELKARTEK), and in part by the Spanish Government (Project PHANTOM) (MCIU/AEI/FEDER, UE) under Grant RTI2018-099162-B-I00.

ABSTRACT Industry 4.0 and Industrial Internet refer to the expected revolution in production, utility management and, in general, fully automated, interconnected and digitally managed industrial ecosystems. One of the key enablers for Industry 4.0 lies on reliable and timely exchange of information and large scale deployment of wireless communications in industry facilities. Wireless will bring solutions to overcome the main drawbacks of the current wired systems: lack of mobility, deployment costs, cable damage dependency and scalability. However, the strict requirements in reliability and latency of use cases such as Factory Automation (FA) and Process Automation (PA) are still a major challenge and a barrier for massive deployment of currently available wireless standards. This paper proposes a PHY/MAC wireless communication solution for FA and PA based on Non-Orthogonal Multiple Access (NOMA) in combination with the 802.11n standard. The communication system proposed aims at delivering two different sets of services. The first service class is composed of Critical Services (CS) with strict restrictions in reliability and latency. The same communication system should convey also a second group of services, referred as Best Effort (BE) with more relaxed boundary conditions. The proposal theoretical background, a detailed transmission-reception architecture, the physical layer performance and the MAC level system reliability are presented in this paper. The solution provides significantly better reliability and higher flexibility than TDMA systems, jointly with a predictable control-cycle latency.

INDEX TERMS 802.11, Factory Automation, IWSN, local area networks, NOMA, P-NOMA Process Automation.

I. INTRODUCTION

The fourth industrial revolution is driving the research and the development in the field of industrial communications. One of the expected trends is the progressive deployment of wireless interconnections as well as global automation for improving efficiency in the use of resources and the integration between processes and factories [1]–[4]. Even though, wired connections are still ruling the majority of the industrial environments. The main reason is the uncertainty of current wireless standards for guaranteeing the tight requirements posed by industrial use cases.

As a paradigmatic example, the 802.11 family of wireless standards was not designed for industrial communications. Nevertheless, they have emerged also as a candidate for industrial applications because of their wide range of available devices, network deployments and applications in practically all communication fields. A major advantage of 802.11 relies on its similarity in OSI layer architecture and compatible protocol structure with Ethernet. This fact provides a high level of interoperability and ensures simple implementation of Ethernet/WLAN internetworking functions. On the weak side, its medium access mechanism, CSMA/CA, does not guarantee deterministic behavior. This fact is a major drawback for real-time services in networks where a massive number of nodes are potentially operating in a crowded spectrum environment [5]. In addition, the standard lacks efficiency for traffic profiles associated to industrial wireless communications (short packets) [6].

A typical Industrial Wireless Sensor Network (IWSN) is depicted in Fig. 1. A generic control system with specific performance and control cycle requirements is assumed.

The associate editor coordinating the review of this manuscript and approving it for publication was Giovanni Pau.

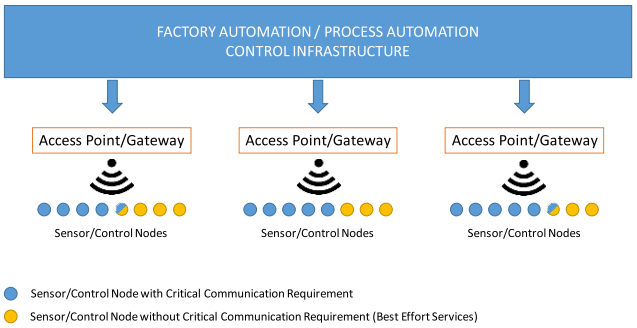

FIGURE 1. Typical industrial wireless sensor network in an industrial environment.

The control system has several access points/gateways (AP) that will serve a set of sensor/control nodes. The distinction of sensor and control functions will be associated to uplink and downlink capabilities of each node. There will be two types of nodes depending on the services associated. Some nodes will be linked to critical services (CS), with strict performance and latency restrictions. Others will not present tight restrictions and will be served on a best effort (BE) basis. Moreover, nodes receiving CS traffic could also be BE receivers. Additionally and in line with performance/latency restrictions, CS and BE service throughput requirements will also be different. In consequence, it is expected that the wireless connection will carry services with orthogonal requirements.

This unbalanced traffic scenario is the perfect operating point for Non-Orthogonal Multiple Access (NOMA) techniques and especially for Layered Division Multiplexing (LDM) [7], a specific power domain NOMA (P-NOMA). LDM has proven better reliability and throughput than the traditional TDM/FDM resource allocation schemes [8]. There are already preliminary proposals in literature for applying NOMA to industrial communications. In [9], authors calculate the robustness and capacity of an ideal NOMA system based on Shannon capacity. However, this work does not provide a complete architecture description in combination with existing standards (PHY and MAC layers) and does not consider specific modulation and coding schemes (MCS), neither provides the combined performance of a PHY and MAC layer. Then in [10], a cross-layer is design to be used between the physical and the data link layers to enhance the energy efficiency in downlink NOMA wireless networks for Visible Light Communication (VLC). Nevertheless, the analysis is carried out adapting the coding and the modulation without considering the integration in any standard and the reliability performance is not studied. In [11], a NOMA-based 802.11n PHY approach is presented and tested in some scenarios. However, no MAC layer is used to provide a realistic industrial communication and the results presented do not reach the low Packet Error Rate (PER) values required the industry.

Aiming at flexibility, capacity and reliability in wireless industrial applications, the present paper proposes the joint use of NOMA/LDM and 802.11n. Although this paper proposes a viability analysis using the well-stablished 802.11n standard, this proposal will be applicable for future versions, such as 802.11ax and 802.11be. The technical contributions of this paper include:

1. To our best knowledge, this paper is the first comprehensive system design and analysis of a NOMA-based 802.11n architecture for industrial communications. A fully detailed explanation of the transmitter and receiver chains is provided, and in addition, the modification that have been assumed in order to make it compatible with the current 802.11n are also included.
2. The proposal gathers also for the first time, in a single framework, the principal steps that any technology has to overcome during the first phase of the standardization process: theoretical background and evaluation, design of the architecture, computer based simulations at PHY and MAC level and network evaluation.
3. A specific MAC layer superframe schedule is designed and evaluated to cope with the specifications of a NOMA-based service delivery.
4. The evaluation of each Key Performance Indicator (KPI) has been carried out according to strict conditions close to real applications. In particular, extensive simulations have been run in order to obtain PER values up to 10^{-3} on the physical layer and 10^{-9} at MAC level. The main reason for this demanding evaluation is to facilitate the possible know-how transfer to industry in the near future.

The paper is organized as follows. The next section describes the characteristics and requirements of industrial communications, as well as the description of two typical industrial scenarios. Section III provides an overview of the system proposal based on 802.11n and NOMA. Section IV discusses necessary modifications in the PHY in order to use NOMA with the 802.11n and the proposal is evaluated in terms of reliability. Section V introduces a deterministic MAC layer based on Time Division Multiple Access (TDMA) to evaluate the PHY proposal in combination with retransmission techniques. Then, in section VI the PHY/MAC proposal is tested in a realistic use case describing the system network performance. Finally, Section VII contains the main conclusions.

II. INDUSTRIAL COMMUNICATION TECHNOLOGIES AND REQUIREMENTS

This section presents the main wireless solutions for industrial communications and the possible use cases.

A. WIRELESS TECHNOLOGIES

According to available literature, such as [12], 802.11 and 802.15 are the most common building blocks in proposals for wireless industrial communications.

802.15 is a working group inside the IEEE 802 specialized in Wireless Personal Area Networks (WPAN) [13]. 802.15 standards are focused on low energy, low-range,

low-data rate, and multi-hop topologies; thus, they are a suitable family for building industrial wireless sensor networks. In addition, the standard supports a deterministic access scheme that provides a bounded latency [14]. However, their usability is commonly limited to monitoring applications due to their low data rate, modest PER, and relatively large latencies [15]. Some wireless networks for industry process monitoring have been effectively implemented using 802.15.4. For instance, [16] presents an 802.15.4-based network for predictive maintenance of manufacturing installations and railway transport. In [16], the authors point out that 802.15.4 can hardly be applied for strict control or safety applications for latency and reliability concerns. Some other works try to improve the feasibility of 802.15.4 for control applications. In [17], a wireless network build with 802.15.4 and a custom TDMA MAC is presented. The TDMA MAC optimizes the network delays and minimizes the cycle time. However, the minimum achievable cycle time was in the 10 ms order, which is out of several industrial applications [18], [19] and they do not mention the achieved PER.

802.11 has been also considered for industrial communication applications. Compared to the 802.15 family, 802.11 provides higher throughput and range. In 2009, the IEEE standardization committees released the standard version IEEE 802.11n [20], which offers up to five times faster transmission modes in comparison with its predecessor, especially due to the introduction of Multiple-Input Multiple-Output (MIMO) systems [21]. Authors in [6] have tested it on real-time industrial communications and the outcome has been a set of guidelines and recommendations in terms of reliability and latency. However, reliability values are only presented up to PER values of 10^{-1}, which is far away from typical industrial performance requirements and it is not realistic to extrapolate those values to very low PER values taking into account the high variance of the industrial wireless propagation channels. Recently, cross layer approaches are a matter of discussion, not only from a PHY-MAC point of view, but also from the network layer perspective. In [22], authors detail different key design aspects in ultra-high-performance wireless networks for critical industrial control applications but unfortunately no simulations results were included. Finally, in [23], SHARP (Synchronous and Hybrid Architecture for Real-time Performance) is presented, a new architecture for industrial automation. Its wireless part includes a novel PHY layer based on 802.11g and integrated in a TDMA MAC structure in order to guarantee deterministic behavior. In this case, convolutional codes are used as channel coding, which are far away from the reliability performance of the LDPC codes introduced in 802.11n.

In summary, the solutions presented so far do not meet the strict industrial requirements and although the 802.11 standard family seems to be more prepared to be integrated in the industry, it cannot be still considered the optimum technology.

B. USE CASES AND SCENARIOS

This paper addresses two industrial communication application use cases: Factory Automation (FA) and Process Automation (PA).

FA refers to industrial communication environments where either individual machines or complete systems require real-time control. These cases are related to production chains, where machines are fundamental elements of the process. Some representative examples would be assembly, packaging, palletizing and manufacturing. Due to the critical role of communications in their respective processes, depending on the application, they require bounded latencies (0.25-10 ms) and Packet Loss Rate (PLR) in the range of 10^{-7}-10^{-9}. In addition, the update time is between 0.5-50 ms and coverage areas are usually well below 100 meters [24], [25].

PA refers to industrial communications for monitoring and diagnosing applications. Examples of PA typical fields are heating, cooling, stirring, and pumping procedures and, in general, machinery condition monitoring. A major difference with FA is the variation speed of measurements and control cycle latency requirements. Most representative values of latency and reliability are within the ranges of 50-100 ms and 10^{-3}-10^{-4} packet loss rate, respectively. Moreover, an update time of 0.1-5 seconds is usually required. Communication ranges are larger than in FA and may vary between 100 and 500 meters [24], [25].

In this work, two deployment scenarios are proposed for system evaluation purposes. In both cases, two services are expected: one critical service (CS), and one non-critical service that will be referred as best effort (BE) service. On the one hand, both PA and FA services will be regarded as critical (CS) even though their requirements in terms of latency and reliability will be different. On the other hand, BE services will not have latency and reliability restrictions and will be applicable in any scenario and use case.

The scenarios provide boundary conditions such as number of nodes, bitrate allocated to each service, service area dimensions and propagation channel characteristics. Scenarios and associated parameters have been based on reference models and experimental data available in [26] and [27] and are gathered in TABLE 1. On the one hand, scenario A represents a relatively large manufacturing hall, with 3200 sq. meters (80×40 m). We assume up to 100 nodes randomly distributed throughout the hall. The access point/gateway will be installed in an optimal position, where LOS and partially obstructed Fresnel zone conditions dominate. On the other hand, Scenario B represents a manufacturing cell, with limited dimensions (10×10 m), up to 20 nodes per cell and NLOS reception conditions. In both cases, a typical manufacturing environment is emulated with plenty of metallic structures and moving machines and staff. The propagation channel (CM 7 or CM 8) choice associated to each environment has been based on [28] and the experiments carried

out on [26]. TABLE 1 summarizes the main parameters and values of each case.

TABLE 1. Use cases and application scenarios.

Parameter	Scenario A Manufacturing Hall	Scenario B Manufacturing Cell
Application	PA	FA
Dimensions (m)	80 x 40 x 10	10 x 10 x10
Number of Nodes	Up to 100	Up to 20
Critical Services (Mbps)	24	12
Non - Critical Services (Mbps)	Up to 48	Up to 48
Channel Model (IEEE 802.15.4)	CM7	CM8

The service capacity requirements associated to the critical services have been differentiated in each scenario. Scenario A has higher number of nodes and lower PER requirement, whereas Scenario B presents less nodes, lower distances and requires a very low PER. Consequently, we have chosen a bitrate capacity close to 24 Mbps for the critical service, whereas this number is reduced to 12 Mbps for the manufacturing cell in scenario B. In both cases, the target throughput of the BE services is 48 Mbps.

III. NOMA-BASED 802.11n

This section introduces the basic principles of NOMA and the requirements for its integration within the 802.11n standard.

A. NON-ORTHOGONAL MULTIPLE ACCESS (NOMA)

Power domain NOMA has recently been successfully applied to broadcast communications [29]. P-NOMA is very efficient in providing different levels of robustness to different services within the same RF channel. This makes the technology an adequate candidate for multiplexing services with unbalanced requirements in industrial wireless applications.

NOMA consists of a signal ensemble composed of several layers, each one taking a portion of the total power delivered by the transmitter. Each layer is configured targeting different robustness levels, decoding thresholds and capacities. The configuration is a function of the modulation/coding choice and the power assignment to each layer. The power splitting is described by Δ (injection level, measured in decibels). The concept of multiplexing two services with NOMA is illustrated in Fig. 2 and the NOMA signal ensemble can be expressed as:

$$x_{NOMA}(k) = x_{CS}(k) + g \cdot x_{BE}(k), \tag{1}$$

where $x_{CS}(k)$ and $x_{BE}(k)$ are the two data streams combined into $x_{NOMA}(k)$ and k is the subchannel index. The injection level g defines the linear power allocation ratio between layers in linear units [7]. This work is based on a two-layer system and, therefore, layers are referred as Upper Layer (UL) and Lower Layer (LL), where CS is transmitted in the UL and BE in the LL, as described in Fig. 2. Due to the power splitting, each service is delivered with less power than in the single-layer case and the power allocated to each

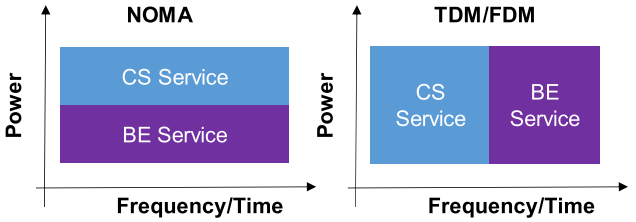

FIGURE 2. Non-Orthogonal and Orthogonal Multiplexing (OM) schemes sharing both the time and the frequency resources.

service can be calculated as:

$$\sigma_i = \frac{10^{\frac{\Delta_{i-1}}{10}}}{\sum_{i=1}^{N} 10^{\frac{\Delta_{i-1}}{10}}}, \tag{2}$$

where, σ_i is the power allocation ratio for layer i (i.e., $i = 1, 2$), N is the total number of layers in the signal ensemble (i.e., $N = 2$) and Δ is the injection level in dB.

The idea of multiple signals on the same channel with unequal error protection was described time ago by some information theory papers such as [30]. The currently available advances in forward error correction make NOMA feasible in real systems. The performance of latest LDPC codes, for instance, is less than half a dB away from the Shannon limit [31]. The second driver for feasibility is the implementation of the signal cancellation structure proposed in [6], which reduces significantly the complexity of the receiver [32]. In [6], a comprehensive comparison of the spectral efficiency of NOMA and traditional TDM/FDM schemes was presented. It is proven that provided the service reception thresholds are unbalanced, the overall gain offered by NOMA can be up to 3 bps/Hz. In practice this gain can be invested in two benefits: 30% higher throughput compared to TDMA solutions [33], [34] or a considerable PER reduction [35]. NOMA will always outperform TDM/FDM, provided an efficient enough channel coding mechanism is used.

Industrial communication systems are typically rolled out for supervision and control purposes, where security, reliability and delay will be critical design constraints. NOMA addresses both security and reliability directly by operating close to zero and even with negative reception thresholds for the most challenging scenarios. Flexible configuration of layers is also an advantage for increasing the security of the PHY. Moreover, processing time and complexity at the receiver are key for system feasibility in industrial environments. The cancellation associated to additional layer decoding involves additional processing latency on the receiver. However, the CS is not affected by this inconvenience as it is transmitted in the UL. Even though, the selected error coding technique for the physical layer waveform will be very important for the Successive Interference Cancellation (SIC) delay [36]. In [32], for instance, the latency associated to large LDPC codes was analyzed. The results show that the number of iterations of the LDPC decoding algorithm remains lower than 5 for Signal-to-Noise Ratio (SNR) values below 4-5 dB,

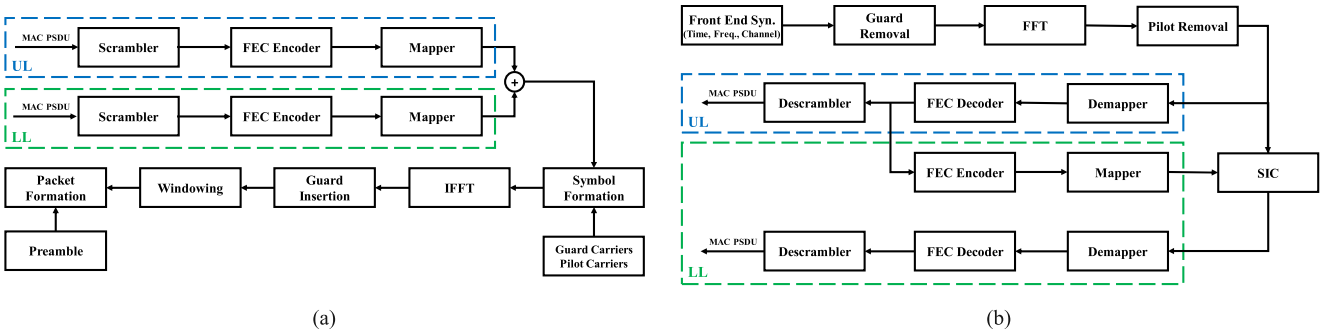

FIGURE 3. General block diagram of the proposed transceiver: (a) NOMA-based 802.11n transmitter, (b) NOMA-based 802.11n receiver.

making the associated decoding time not relevant on the overall OFDM receiver processing time budget, mostly influenced by MAC operations [32]. It should be noted that time requirements cannot be described on a general basis. Each application scenario requires a thorough analysis of the control-cycle vs. receiver processing time.

B. NOMA ON 802.11n

A new communication architecture based on modifications to the PHY of the 802.11n standard in order to include NOMA is presented in this subsection.

First, at the MAC layer, the LL Physical Service Data Unit (PSDU) packet length is adjusted according to the UL length in order to ensure that both components, UL and LL, will make use of the same number of symbols per frame in the physical layer. This adaptation will enable the use of a simplified NOMA mapping block, which will be included immediately after the combination of individual mappers plus an amplitude adaptation operation (injection level). Consequently, the LL receiver complexity will be greatly reduced. Previous work already assessed the relevancy of a proper choice of the data overlapping for efficient and simple receiver implementation [32]. In particular, the length of the BE PSDU can be calculated as:

$$PSDU_{BE} = \left\lfloor \left(Sym_{Num(CS)} * NDBPS_{BE} - N_{Service} \right) / 8 \right\rfloor \quad (3)$$

where, $Sym_{Num(CS)}$ is the number of complex symbols required for the CS, $NDBPS_{BE}$ is the number of coded bits per OFDM symbol of the BE service and $N_{Service}$ is the number of bits in the service field.

In fact, if the system uses OFDM and the framing structure of each one of the layers are synchronized, the receiver complexity and latency are limited. The mapping and framing stage are inherited directly from 802.11n MCS. The only difference is that both services are combined into a single stream after mapping (see Fig. 3 (a)). To do so, the complex symbols corresponding to the LL are attenuated by a predefined injection level. The injection level in linear units (i.e., g) indicates the relative power distribution between both layers, so g has a real value within the range [0, 1), where $g = 0$ results in a single-layer system and $g = 1$ results in a two-layer system with equal power distribution. Then, the UL and the attenuated LL are added creating the definitive NOMA signal ensemble. After superimposing both layers, the output constellation is normalized. In this particular case, the UL is in charge of delivering CS content, while BE content is mapped into the LL. Once both services are combined into a single P-NOMA signal ensemble, both services will undergo the same processing stages. The final physical waveform is then sent in the form of PHY packets composed of a preamble and a data field. The detailed structure of the PHY packet is maintained as defined in 802.11n.

The first modules of the NOMA receiver are identical to those on current 802.11n receivers (See Fig. 3 (b)). After RF conditioning, the carrier and time synch stages prepare the input for channel and equivalent noise estimation.

Then a Least Square (LS)-based equalization is performed and the CS goes through decoding, demapping and descrambling stages. The CS bit stream will be available for all sensor/actuators of the service area without additional complexity since the lower layer will be assumed as additional noise for the UL. If the available SNR permits, the cancellation and lower layer decoding will be the next steps. The cancellation will depend on the injection level, the channel estimation metrics and the CS itself. At the receiver, the NOMA ensemble on the k-th channel can be expressed as:

$$y_{NOMA}(k) = \left(x_{CS}(k) + g \cdot x_{BE}(k) \right) \cdot h(k) + n(k), \quad (4)$$

where $y_{NOMA}(k)$ is the received symbol, $h(k)$ is a static multipath channel and $n(k)$ is the sum of AWGN noise and other additive interference. CS can be accessed as usual without any further requirements. Once the UL has been decoded, a signal cancellation algorithm provides access to the BE. In this work, for the signal cancellation stage the Hard-SIC cancellation scheme is proposed due to its good trade-off between complexity and performance. In particular, the same Hard-SIC cancellation mechanism has been adopted by receivers of latest Advanced Television Systems Committee (ATSC) digital TV standard, ATSC 3.0, showing a successful balance between complexity and performance [29]. The decoded CS layer is coded and modulated again, and then, it is removed from the equalized NOMA signal

(See Fig. 3 (b)). After these stages, the received signal can be expressed as:

$$\tilde{x}_{BE}(k) = g \cdot x_{BE}(k) + i(k) + n(k), \quad (5)$$

where $i(k)$ is the error cancellation due to the channel estimation error and $\tilde{x}_{BE}$ is the obtained BE data [6]. Eventually, the obtained signal goes through the same decoding, demapping and descrambling stages as the CS.

C. CAPACITY COMPARISON

The purpose of this section is to demonstrate theoretically that the inclusion of NOMA in 802.11n standard provides an increase of the system capacity. Fig. 4 shows the capacity gain of NOMA for different configurations. The x-axis represents the percentage of time dedicated to the delivery of CS content, while the y-axis is the capacity gain obtained as the difference between the optimum TDM configuration throughput and the optimum NOMA throughput. The different curves imply different restriction on the maximum SNR value that CS and BE services can assume. Based on those values the optimum MCS configuration is carried out for both technologies.

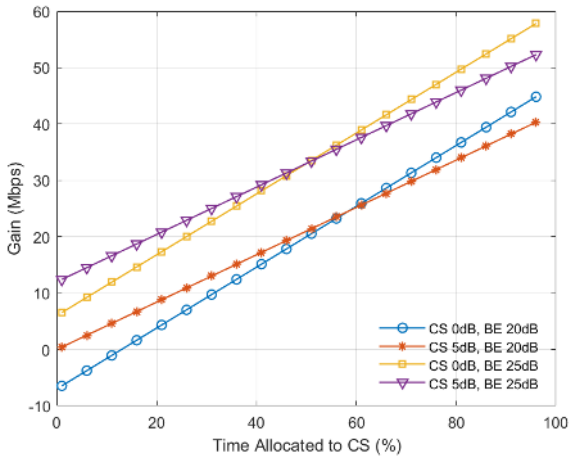

FIGURE 4. Potential gain using NOMA in combination with 802.11n.

Firstly, Fig. 4 shows that in the majority of the cases, NOMA offers a considerable capacity gain with maximum values between 40-60 Mbps. The gain increases linearly proportional to the percentage of time allocated to CS, where the higher are the time requirements of CS, the higher is the gain that NOMA can offer. In addition, the curves present different gradient due to the performance of NOMA. In fact, the higher is the asymmetry between the SNR requirements of the services, the higher is the gradient of the grain that NOMA can offer. Finally, it should also be remarked that for the low values of time percentage allocated to CS, NOMA does not provide enough gain, and so, TDM could be a better solution. However, taking into account the industrial time requirements, cases where the majority of the time are allocated to non-critical services are not very representative. The main reason is that service configuration is carried out to meet the strict requirements of CS and, therefore, a low percentage of time dedicated to CS may indicate that the service configuration is not optimized.

D. PROPOSED CONFIGURATIONS

Based on the scenarios described in previous sections, two different configurations are proposed for each of the multiplexing schemes. On the one hand, in the NOMA-Config. A (PA), the UL is targeting a CS with a throughput of about 24 Mbps (MCS1), whereas the LL is delivering 48 Mbps (MCS3) as a BE service and the injection level is −10.5 dB. In NOMA-Config. B (FA), the UL is decreased to 12 Mbps (MCS0) and the injection level to −10 dB in order to satisfy the more tight requirements of FA, while the EL configuration remains the same. PHY configurations are summarized in TABLE 2.

TABLE 2. PHY configurations.

		NOMA	TDM
PA - Scenario A	Config. A CS (24 Mbps) BE (48 Mbps)	QPSK 1/2 16QAM 1/2	16 QAM 1/2 64QAM 2/3
FA - Scenario B	Config. B CS (12 Mbps) BE (48 Mbps)	BPSK 1/2 16QAM 1/2	QPSK 1/2 64QAM 2/3

On the other hand, the resources are always 50%-50% shared by both service types in TDM/FDM configurations. In the first case, TDM-Config. A, the MCS3 is proposed for the CS, whereas for the second scenario TDM-Config. B the MCS1 is enough to satisfy the minimum CS throughput. Eventually, in both cases the BE data is conveyed with MCS5 and a throughput of 48 Mbps. The packet length of the CS service has been configured to deliver a payload of 18 bytes.

IV. PHYSICAL LAYER (PHY)

This section provides guidelines for the design of the proposed PHY layer and presents the performance analysis.

A. DESIGN

The potential gain of the NOMA proposal has been studied by through simulations of the complete physical layer [37], [38]. A prototype transmitter and receiver chain has been implemented for this purpose. This prototype is compliant with the 802.11 a/g/n standard and includes modifications to enable NOMA multiplexing capabilities as described in Section III (See Fig. 3).

The system evaluation set up has included two industrial propagation models for performance evaluation purposes: the CM 7 (Scenario A) and CM 8 (Scenario B) channel models [28]. Considering this work as a feasibility analysis of the upper limit of the potential gain provided by NOMA to 802.11n, perfect synchronization and channel estimation are assumed. Access the Lower Layer is granted after SIC cancellation as explained in Section III.B. In line with the ideal

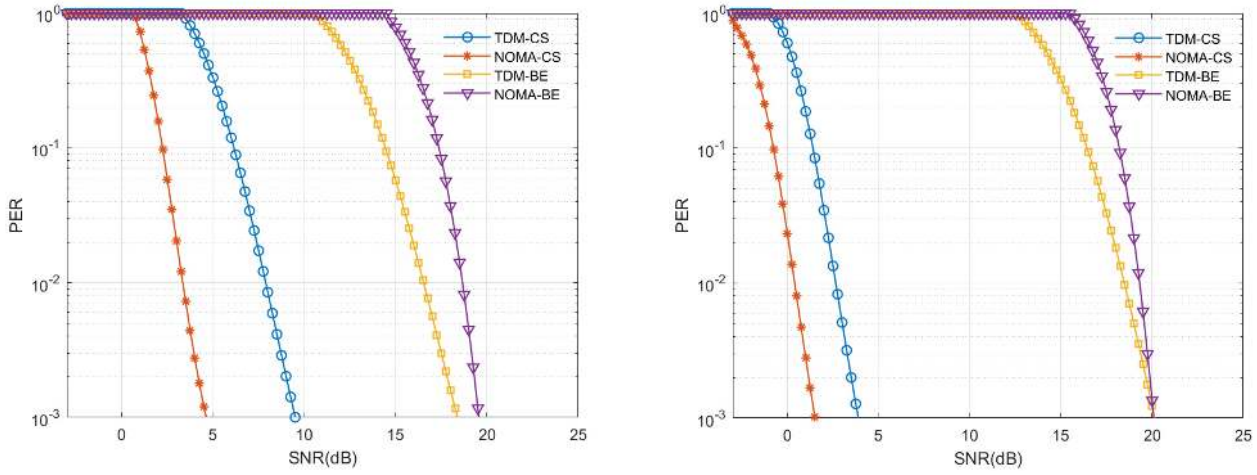

FIGURE 5. Performance results for the PHY layer: (a) Scenario A (b) Scenario B.

synch and estimation considerations, cancellation has been also considered ideal. Previous works have demonstrated that it is possible to keep the cancellation noise below the system AWGN [7], [39].

The PHY performance has been evaluated using. This is one of the key performance indicators in industrial applications (a PSDU packet is considered erroneous if any of the bits are decoded incorrectly). The number of simulated packets and the SNR simulation steps have been adapted to the expected PER values. In particular, the simulated packet number is always at least one order of magnitude higher than the required value for obtaining the desired PER value assuming one single error. In addition, for the best granularity the lower PER values are calculated within 0.25 dB steps. The obtained results are fed to OMNeT++ as the PHY error model.

B. EVALUATION

As part of the proposal study, the PHY performance of configurations proposed in Section III.D are displayed in Fig. 5 (a) and Fig. 5 (b) for Scenario A and Scenario B, respectively. The receiving thresholds at the physical layer are limited to PER $= 10^{-3}$. It must be noted, that the MAC level retransmissions, even limited for latency considerations, will bring PER values down to 10^{-8}.

The UL gain in Fig. 5 (a) is close to 5 dB, whereas the LL performance is within a 1.5 dB margin for both multiplexing schemes. In Fig. 5 (b), however, the NOMA UL gain is reduced to about 2.5 dB and the LL performance is even closer. The relevance of the result lies on the significant gain in PHY performance, close to 5 dB gain for a very challenging scenario, which will provide room for flexible MAC design. The reason for this gain is that in order to compensate the capacity reduction in TDMA systems because of the resource sharing between CS and BE, higher modulation orders have to be used in comparison with NOMA. Therefore, more robust configurations can be used in NOMA, while the same capacity as in TDMA is offered.

V. MAC LAYER DEFINITION AND PERFORMANCE

This section presents the design of the proposed MAC layer and the performance analysis.

A. DESIGN

In this section, a specific MAC layer for implementing the NOMA-based 802.11n PHY proposal is presented. This MAC layer proposal combines in the same time schedule the NOMA signal ensemble with a TDMA medium access technique to guarantee deterministic packet delivery and a packet retransmission scheme in the time domain to increase the reliability. Additionally, it is assumed that the nodes share a common time reference that allows guaranteed access to the medium without any interferences, such as [40], [41]. In order to measure the benefits of introducing NOMA, a single-layer TDMA MAC with packet retransmission schemes has been designed and implemented. Both MAC layer superframe structures, TDMA and NOMA + TDMA, are presented in Fig. 6.

Both superframe structures are composed of four different periods: CS transmission, uplink feedback, on-demand retransmissions and BE period. During the CS transmission period, the AP sends the corresponding CS information to each slave in a dedicated time slot. Then, in the uplink feedback period, each slave sends an ACK packet if the CS has been correctly received or NACK packet if the CS has not been correctly received. The ACK/NACK packet transmission is carried out in single-layer mode in both cases, TDMA and NOMA. In the on-demand retransmission period, each of the requested retransmissions in the previous period is carried out by the AP in another dedicated time slot. To define

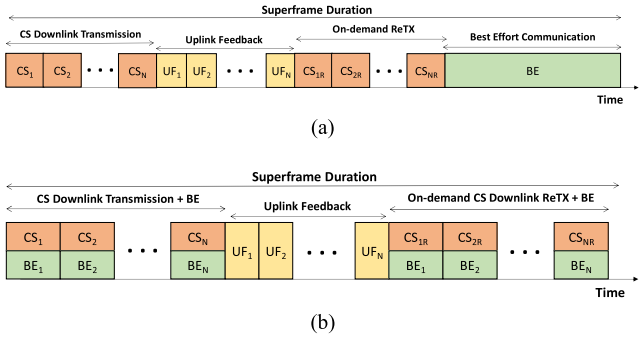

FIGURE 6. Superframe time representation: (a) TDMA, (b) NOMA + TDMA.

the duration of this period, the worst possible case is assumed, that is, one slot per each CS packet retransmission is reserved. Finally, in the BE period non-critical information is delivered. The length of each period depends on the MCS on use. The lower the MCS is, the higher the required transmission time is, and so, the longer the period is. Taking into account the PHY configurations (TABLE 2), since NOMA uses lower MCS values, NOMA periods are longer than TDMA periods for the same packet lengths.

The main difference between the two superframe structures is that by using NOMA, BE services are delivered in the LL. On the one hand, this effect reduces the superframe time duration since only three periods have to be reserved in the time domain. On the other hand, as NOMA techniques are implemented in combination with a deterministic TDMA structure, BE services are transmitted in the lower layer aligned with CS. In consequence, it will be much easier to determine the timing of the transmission and the reception of each BE packet since the determinism obtained by the use of TDMA is also applied to the BE services. The consequence is an easier prediction of latency also for BE services. Another advantage of the simultaneous delivery of CS and BE services is that when a retransmissions are required for CS, the BE packet is also retransmitted, and so, a second chance is obtained for the correct reception of BE traffic.

B. EVALUATION

In order to evaluate the reliability of the proposed MAC layer, the OMNeT++ network simulator has been used [42]. The designed MAC layer has been implemented in combination with the PHY configurations described in the previous section. The scenarios (A and B) described in section II.B have been used (see TABLE 1). The number of nodes in the network has been set initially to 50 in scenario A and 10 in scenario B. Later, the impact of increasing the number of nodes and the maximum slots of a TDM/NOMA superframe as a function of T_{cycle} will be calculated.

Firstly, the superframe length is different for each technology and configuration. Therefore, the minimum T_{Cycle} would also be different, since in this work, the T_{Cycle} is assumed as the minimum required time to carry out all the required communications described in the superframe (i.e., the superframe length), which means that the lower the T_{Cycle}, the faster are the slaves updated. In particular, for the same number of nodes, NOMA superframes are shorter than TDM superframes. In fact, TDM superframe is 22% and 17.5% longer than NOMA superframe in scenario A and scenario B, respectively.

In Fig. 7, CS reliability curves obtained from the MAC evaluation are presented in terms of PER and PLR vs. SNR. This work assumes PER as the error rate without retransmissions and PLR as the error rate after implementing retransmissions. Regarding the performance obtained in scenario A (Fig. 7 (a)), NOMA-based MAC offers better results than TDM for restrictive PER and PLR values (i.e., 10^{-9}). In particular, NOMA performs 2.5 dB better than TDM in terms of PLR and more than 6 dB in terms of PER.

If the impact of the retransmission schemes is individually analyzed, the relative reliability improvement achieved in TDM is higher than in NOMA (i.e., 7dB vs. 4 dB). The difference on the impact of the retransmissions is associated to PHY configurations in each case, as TDM uses a less robust MCS, retransmissions are more effective. Similar reliability results are obtained in Fig. 7 (b) for scenario B. In this case, the gain that NOMA-based system offers in comparison with TDM system is 2.3 dB and 1.7 dB in terms of PLR and PER, respectively. In general, performance values are better in scenario B since more robust configurations are implemented for the CS.

The PER performance of the BE component is presented in Fig. 8. In the case of scenario B, performance results are very similar in both cases, the difference is lower than half dB. However, in scenario A TDM offers slightly higher reliability (around 3 dB). Nevertheless, the reliability difference for both technologies is not as critical as in the case of CS. Moreover, PLR results of the NOMA MAC layer are not included in Fig. 8 since they are very similar to the PER values. The main reason for this effect is the short time interval between the transmission and the retransmission, usually much shorter than channel time coherence.

VI. COMPREHENSIVE NETWORK EVALUATION

In this section, the PHY layer (Section IV) and the MAC (Section V) are combined based on the scenarios detailed in Section II.B. The objective of this study is to test the proposed solution in terms of reliability and latency in a realistic network. Simulations have been carried out in OMNeT++. The system uses a 40 MHz channel bandwidth in the 2.4 GHz ISM band, −90dBm is the thermal noise power and the transmitted power is set to 10 dBm. It is assumed that the nodes are randomly distributed along the network. The path loss model includes the free space path losses plus a shadowing component that is characterized with a log-normal distribution with mean zero and $\sigma = 6$ dB [43]. A summary of the parameters is presented in TABLE 3.

Fig. 9 shows the results of reliability associated to each scenario. Scenario A and Scenario B are presented independently in Fig. 9 (a) and Fig. 9 (b), respectively. In general,

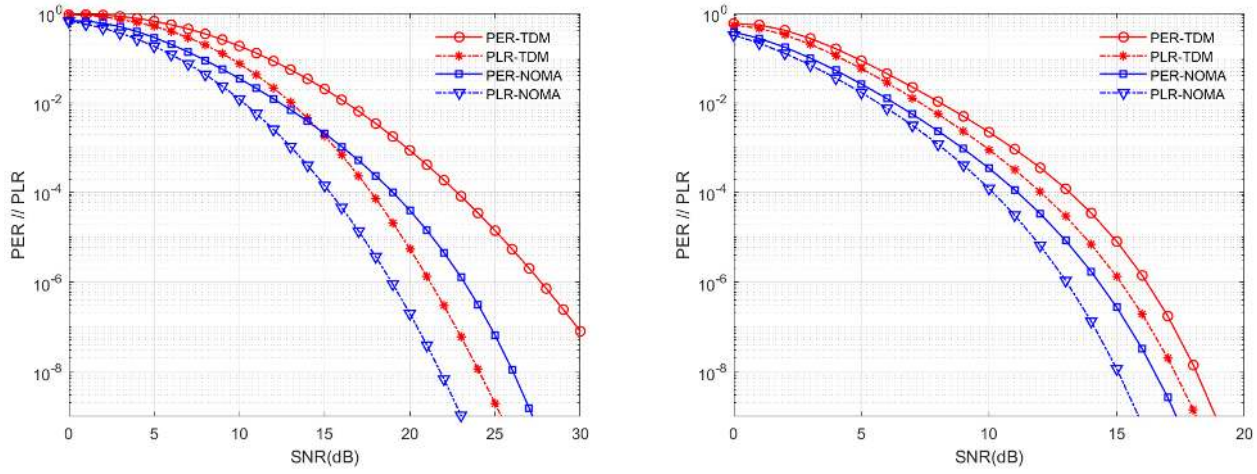

FIGURE 7. MAC layer CS reliability results: (a) Scenario A, (b) Scenario B.

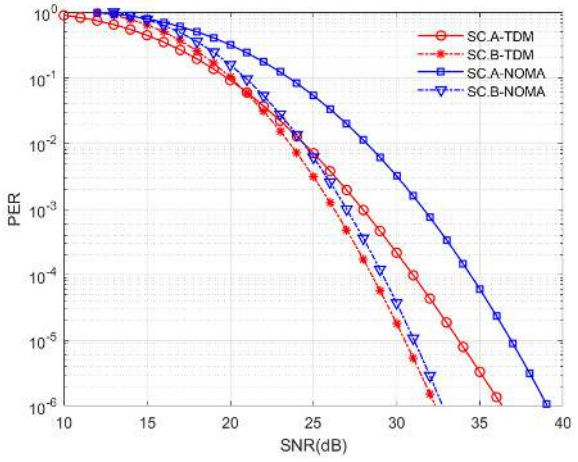

FIGURE 8. MAC layer BE reliability results.

TABLE 3. Simulation parameters.

Parameter	Value
Center Frequency	2.4 GHz
Bandwidth	40 MHz
Noise Power	-90 dBm
Transmitted Power	10 dBm
Shadowing	Mean = 0 dB σ = 6 dB
Number of Nodes	50 in Sc. A 10 in Sc. B
Channel Model	CM7 in Sc. A CM8 in Sc. B
Network Size	80 x 40 m^2 in Sc. A 10 x 10 m^2 in Sc. B
CS data rate	24 Mbps in Sc. A 12 Mbps in Sc. B
BE data rate	48 Mbps

NOMA offers considerable better performance for the CS. In fact, in all CS cases (see Fig. 9), NOMA outperforms TDM in at least one order of magnitude. In particular, PLR values below 10^{-8} are obtained using NOMA. On the other hand, looking at BE services, TDM offers slightly better performance results than NOMA in Scenario A, while in Scenario B, results are very similar for both technologies. In addition, to the reliability results, the effect of the error packets and the retransmissions over the received throughput is presented in TABLE 4. As in the case of reliability results, NOMA provides a better use of system data capacity for CS services as results appear closer to the maximum (i.e., 24 Mbps in scenario A and 12 Mbps in scenario B) results. On the contrary, regarding the received effective throughput related with BE services, TDM-based architecture provides slightly better results, although, in both cases, the throughput decrease is assumable taking into account the characteristics of BE services. In summary, in order to improve the reliability of CS by using NOMA, a tradeoff has to be assumed between the performance of the CS and the BE.

Concerning time requirements, an end-to-end (E2E) latency analysis is presented in TABLE 5. NOMA can assume lower T_{Cycle} values while carrying out the same services as in TDMA. Then, the minimum E2E latency is defined as the time required to deliver a CS data packet. As expected, the minimum latency of NOMA is higher than the minimum latency of TDM because it uses lower MCS in the PHY configuration. The maximum latency is obtained when the CS packet is received in the on-demand retransmission period. Again, the different MCS choices cause different maximum values. Finally, the last column in TABLE 5, presents the mean latency obtained from the simulation of all the scenarios. In general, mean values are very close to the minimum latency values in all cases. This means that few retransmissions have been required to deliver the CS information correctly. However, the difference between the minimum and the mean latency is lower in NOMA than in TDM, because of its higher reliability. Doubtlessly, results

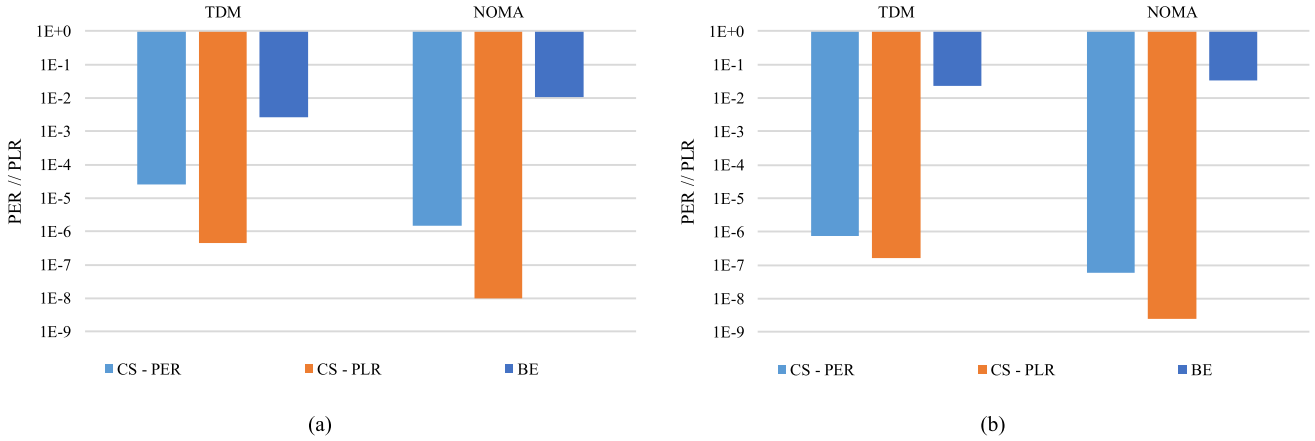

FIGURE 9. Reliability results obtained in: (a) Scenario A, (b) Scenario B.

TABLE 4. Received effective throughput.

	CS (Mbps)	BE (Mbps)
Sc. A - TDM	23.999401	47.869998
Sc. A - NOMA	23.999965	47.478968
Sc. B - TDM	11.999991	46.875871
Sc. B - NOMA	11.999999	46.349872

TABLE 5. E2E latency comparison.

	T_{cycle} (ms)	Min. E2E Latency (µs)	Max. E2E Latency (ms)	Mean E2E Latency (µs)
Sc. A - TDM	10.4	50	5.20	50.13000
Sc. A - NOMA	8.50	58	5.60	58.00500
Sc. B - TDM	2.28	58	1.12	58.00100
Sc. B - NOMA	1.94	70	1.24	70.00003

indicate that NOMA-based systems are more deterministic than TDM systems, since instantaneous latency values are less variable.

The length of the superframe structure is conditioned by the number of nodes that are served in each cycle time. Therefore, depending on the time requirements that have to be guaranteed (maximum cycle time), different number of nodes can be served depending on the multiplexing technology used. TABLE 6 contains the number of nodes that can be included in the designed superframe for different T_{cycle} values. The first two values (100 ms and 50 ms) are related to PA environments, where time requirements are more flexible. Then, the other three values (10 ms, 5 ms and 1 ms) are related to FA environments. In general, by using NOMA, more nodes can be included, specifically, the amount of served nodes can be increased by around 20%. It is worth mentioning the case of a T_{cycle} of 100 ms, where the number of nodes in the superframe is maximum. In this case, by using NOMA 108 extra nodes could be served in scenario A and 77 more in scenario B.

Finally, it is important to highlight that although originally only scenario B is oriented to FA environments (scenario A is oriented to PA), based on the latency and

TABLE 6. Served nodes for different T_{CYCLE} sizes.

	T_{cycle} 100 ms	50 ms	10 ms	5 ms	1 ms
Sc. A - TDM	480	240	48	24	4
Sc. A - NOMA	588	294	58	29	5
Sc. B - TDM	438	219	43	21	4
Sc. B - NOMA	515	257	51	25	5

reliability results obtained in TABLE 5 and Fig. 9, in both scenarios FA applications could be delivered by using NOMA.

VII. CONCLUSION

This article provides a comprehensive proposal of a NOMA-based 802.11n architecture for industrial applications. In addition to the necessary theoretical basis and the specific PHY/MAC NOMA design in combination with 802.11n, realistic requirements and scenarios have been detailed based on PA and FA, where the NOMA-based 802.11n proposal could be implemented. First, a simulation setup has been presented at PHY level in order to test the reliability increase obtained by introducing NOMA in the PHY. Then, a particular MAC layer structure has been presented to manage a deterministic medium access with a useful retransmission scheme. Finally, the performance of the PHY/MAC design has been tested in the described industrial scenarios. Reliability and latency have been the principal KPI.

In general, NOMA offers significantly better reliability results than TDMA. On the one hand, as shown in Section IV, the reliability of the CS is highly increased by using more robust MCS configurations. On the other hand, the robustness increase in the NOMA-based CS is maintained in the MAC layer performance curves. In fact, up to 6 dB of gain can be obtained for PER values of 10^{-9}, since NOMA-based CS can be obtained for a SNR of around 27 dB, while for TDMA around 33 dB of SNR are required. In addition, the effect of the proposed time retransmission scheme is confirmed in both technologies NOMA and TDM, since the required SNR is reduced. It has been observed that in some cases, TDMA-based systems offer slightly better results for BE services, but this fact has not been considered critical for FA or PA scenarios. It is also important to emphasize that

in all the simulated realizations in section VI, an important improvement is obtained PER and PLR metrics for NOMA. In fact, NOMA-based results outperform TDM results in at least one order of magnitude in each of the evaluated cases. In both scenarios, the PLR value obtained by using NOMA is below 10^{-8}. Consequently, a tradeoff has to be assumed between CS and BE, where in order to obtain a considerable gain in the CS, BE services have to assume a little penalization.

Concerning latency analysis, results are more similar between both technologies than in the case of reliability. As presented in section VI, although it is true that minimum and maximum latency values are slightly lower in TDM system, in both cases latency values meet the FA time requirements. However, the mean latency results in NOMA are very close to the minimum latency, which means that the instantaneous latency values are more constant. This effect occurs due to the increase in reliability in NOMA cases and it implies that NOMA-based communications are more deterministic than TDMA-based communications. Moreover, it is important to highlight that due to the superframe structure, more nodes can be included in the NOMA-based superframe than in the TDMA-based superframe for the same T_{cycle}.

Finally, an extra advantage is obtained with NOMA in comparison to TDMA: determinism in BE services. In most cases, absolute latency values are not critical for BE services, but in our proposal, latency of BE services becomes more easily predictable than in TDMA frame structures. Finally, as a future work, it would be interesting to validate this proposal in an industrial environment with real hardware. Hence, how to implement this proposal in commercial devices would be studied for creating compatible transceivers with NOMA technology.

REFERENCES

[1] A. Varghese and D. Tandur, "Wireless requirements and challenges in industry 4.0," in *Proc. Int. Conf. Contemp. Comput. Informat. (IC3I)*, Mysore, India, Nov. 2014, pp. 634–638.

[2] R. Drath and A. Horch, "Industrie 4.0: hit or hype? [Industry Forum]," *IEEE Ind. Electron. Mag.*, vol. 8, no. 2, pp. 56–58, Jun. 2014.

[3] R. Rajkumar, I. Lee, L. Sha, and J. Stankovic, "Cyber-physical systems: The next computing revolution," in *Proc. Design Automat. Conf.*, Anaheim, CA, USA, Jun. 2010, pp. 731–736.

[4] M. Annunziata and P. C. Evans, "Industrial Internet: Pushing the boundaries of minds and machine," in *General Electric*. General Electric Reports, 2012.

[5] Z. Fernandez, C. Cruces, I. Val, and M. Mendicute, "Deterministic real-time access point concepts for industrial hybrid Ethernet/IEEE 802.11 networks," in *Proc. IEEE Int. Workshop Electron., Control, Meas., Signals Appl. Mechatronics (ECMSM)*, Donostia-San Sebastian, Spain, May 2017, pp. 1–6.

[6] F. Tramarin, S. Vitturi, M. Luvisotto, and A. Zanella, "On the use of IEEE 802.11n for industrial communications," *IEEE Trans. Ind. Informat.*, vol. 12, no. 5, pp. 1877–1886, Oct. 2016.

[7] L. Zhang, W. Li, Y. Wu, X. Wang, S.-I. Park, H. M. Kim, J.-Y. Lee, P. Angueira, and J. Montalban, "Layered-Division-multiplexing: Theory and practice," *IEEE Trans. Broadcast.*, vol. 62, no. 1, pp. 216–232, Mar. 2016.

[8] S. M. R. Islam, N. Avazov, O. A. Dobre, and K.-S. Kwak, "Power-domain non-orthogonal multiple access (NOMA) in 5G systems: Potentials and challenges," *IEEE Commun. Surveys Tuts.*, vol. 19, no. 2, pp. 721–742, 2nd Quart., 2017.

[9] E. Arruti, M. Mendicute, and M. Barrenechea, "Unequal error protection with LDM in inside carriage wireless communications," in *Proc. 15th Int. Conf. ITS Telecommun. (ITST)*, Warsaw, Poland, May 2017, pp. 1–5.

[10] S. Murugaveni and K. Mahalakshmi, "A novel approach for non-orthogonal multiple access for delay sensitive industrial IoT communications for smart autonomous factories," *J. Ambient Intell. Humanized Comput.*, to be published.

[11] E. Iradier, J. Montalban, L. Fanari, P. Angueira, O. Seijo, and I. Val, "NOMA-based 802.11n for broadcasting multimedia content in factory automation environments," in *Proc. IEEE Int. Symp. Broadband Multimedia Syst. Broadcast. (BMSB)*, Jeju, South Korea, Jun. 2019, pp. 1–6.

[12] A. Frotzscher, U. Wetzker, M. Bauer, M. Rentschler, M. Beyer, S. Elspass, and H. Klessig, "Requirements and current solutions of wireless communication in industrial automation," in *Proc. IEEE Int. Conf. Commun. Workshops (ICC)*, Sydney, NSW, Australia, Jun. 2014, pp. 67–72.

[13] M. Bal, "Industrial applications of collaborative wireless sensor networks: A survey," in *Proc. IEEE 23rd Int. Symp. Ind. Electron. (ISIE)*, Istanbul, Turkey, Jun. 2014, pp. 1463–1468.

[14] G. Cena, A. Valenzano, and S. Vitturi, "Hybrid wired/wireless networks for real-time communications," *IEEE Ind. Electron. Mag.*, vol. 2, no. 1, pp. 8–20, Mar. 2008.

[15] V. C. Gungor and G. P. Hancke, "Industrial wireless sensor networks: Challenges, design principles, and technical approaches," *IEEE Trans. Ind. Electron.*, vol. 56, no. 10, pp. 4258–4265, Oct. 2009.

[16] K. Das, P. Zand, and P. Havinga, "Industrial wireless monitoring with energy-harvesting devices," *IEEE Internet Comput.*, vol. 21, no. 1, pp. 12–20, Jan. 2017.

[17] M. Anwar, Y. Xia, and Y. Zhan, "TDMA-based IEEE 802.15.4 for low-latency deterministic control applications," *IEEE Trans. Ind. Informat.*, vol. 12, no. 1, pp. 338–347, Feb. 2016.

[18] M. Luvisotto, Z. Pang, and D. Dzung, "High-performance wireless networks for industrial control applications: New targets and feasibility," *Proc. IEEE*, vol. 107, no. 6, pp. 1074–1093, Jun. 2019.

[19] G. J. Sutton, J. Zeng, R. P. Liu, W. Ni, D. N. Nguyen, B. A. Jayawickrama, X. Huang, M. Abolhasan, Z. Zhang, E. Dutkiewicz, and T. Lv, "Enabling technologies for ultra-reliable and low latency communications: From PHY and MAC layer perspectives," *IEEE Commun. Surveys Tuts.*, vol. 21, no. 3, pp. 2488–2524, 3rd Quart., 2019.

[20] *Orthogonal Frequency Division Multiplexing (OFDM) PHY Specification, de Standard—Part 11: Wireless LAN Medium Access Control (MAC) and Physical Layer (PHY) Specifications*, Nueva York, Estados Unidos, IEEE Computer Society, Standard 802.11, 2012, pp. 1583–1630.

[21] J. Lorincz and D. Begusic, "Physical layer analysis of emerging IEEE 802.11n WLAN standard," in *Proc. 8th Int. Conf. Adv. Commun. Technol.*, Phoenix Park, South Korea, Feb. 2006, p. 194.

[22] M. Luvisotto, Z. Pang, and D. Dzung, "Ultra high performance wireless control for critical applications: Challenges and directions," *IEEE Trans. Ind. Informat.*, vol. 13, no. 3, pp. 1448–1459, Jun. 2017.

[23] O. Seijo, Z. Fernandez, I. Val, and J. A. Lopez-Fernandez, "SHARP: A novel hybrid architecture for industrial wireless sensor and actuator networks," in *Proc. 14th IEEE Int. Workshop Factory Commun. Syst. (WFCS)*, Imperia, Italy, Jun. 2018, pp. 1–10.

[24] P. Schulz, M. Matthe, H. Klessig, M. Simsek, G. Fettweis, J. Ansari, S. A. Ashraf, B. Almeroth, J. Voigt, I. Riedel, A. Puschmann, A. Mitschele-Thiel, M. Müller, T. Elste, and M. Windisch, "Latency critical IoT applications in 5G: Perspective on the design of radio interface and network architecture," *IEEE Commun. Mag.*, vol. 55, no. 2, pp. 70–78, Feb. 2017.

[25] S. Dietrich, G. May, O. Wetter, H. Heeren, and G. Fohler, "Performance indicators and use case analysis for wireless networks in factory automation," in *Proc. 22nd IEEE Int. Conf. Emerg. Technol. Factory Autom. (ETFA)*, Limassol, Cyprus, Sep. 2017, pp. 1–8.

[26] R. Croonenbroeck, L. Underberg, A. Wulf, and R. Kays, "Measurements for the development of an enhanced model for wireless channels in industrial environments," in *Proc. IEEE 13th Int. Conf. Wireless Mobile Comput., Netw. Commun. (WiMob)*, Rome, Italy, Oct. 2017, pp. 1–8.

[27] X. Jiang, Z. Pang, M. Luvisotto, F. Pan, R. Candell, and C. Fischione, "Using a large data set to improve industrial wireless communications: Latency, reliability, and security," *IEEE Ind. Electron. Mag.*, vol. 13, no. 1, pp. 6–12, Mar. 2019.

[28] A. F. Molisch, *IEEE 802.15. 4a Channel Model-Final Report*, IEEE Standard P802, vol. 15, no. 4, pp. 1–41, 2004.

[29] S. I. Park, J.-Y. Lee, S. Myoung, L. Zhang, Y. Wu, J. Montalban, S. Kwon, B.-M. Lim, P. Angueira, H. M. Kim, N. Hur, and J. Kim, "Low complexity layered division multiplexing for ATSC 3.0," *IEEE Trans. Broadcast.*, vol. 62, no. 1, pp. 233–243, Mar. 2016.
[30] P. Bergmans and T. Cover, "Cooperative broadcasting," *IEEE Trans. Inf. Theory*, vol. 20, no. 3, pp. 317–324, May 1974.
[31] L. Michael and D. Gomez-Barquero, "Bit-interleaved coded modulation (BICM) for ATSC 3.0," *IEEE Trans. Broadcast.*, vol. 62, no. 1, pp. 181–188, Mar. 2016.
[32] S. I. Park, Y. Wu, L. Zhang, J. Montalban, J.-Y. Lee, P. Angueira, S. Kwon, H. M. Kim, N. Hur, and J. Kim, "Low complexity layered division multiplexing system for the next generation terrestrial broadcasting," in *Proc. IEEE Int. Symp. Broadband Multimedia Syst. Broadcast.*, Jun. 2015, pp. 1–3.
[33] S.-I. Park, J.-Y. Lee, B.-M. Lim, S. Kwon, J.-H. Seo, H. M. Kim, N. Hur, and J. Kim, "Field comparison tests of LDM and TDM in ATSC 3.0," *IEEE Trans. Broadcast.*, vol. 64, no. 3, pp. 637–647, Sep. 2018.
[34] J. Montalban, P. Scopelliti, M. Fadda, E. Iradier, C. Desogus, P. Angueira, M. Murroni, and G. Araniti, "Multimedia multicast services in 5G networks: Subgrouping and non-orthogonal multiple access techniques," *IEEE Commun. Mag.*, vol. 56, no. 3, pp. 91–95, Mar. 2018.
[35] E. Iradier, J. Montalban, L. Fanari, P. Angueira, L. Zhang, Y. Wu, and W. Li, "Using NOMA for enabling Broadcast/Unicast convergence in 5G networks," *IEEE Trans. Broadcast.*, vol. 66, no. 2, pp. 503–514, Jun. 2020.
[36] M. Zhan, Z. Pang, D. Dzung, and M. Xiao, "Channel coding for high performance wireless control in critical applications: Survey and analysis," *IEEE Access*, vol. 6, pp. 29648–29664, 2018.
[37] F. Qin, X. Dai, and J. E. Mitchell, "Effective-SNR estimation for wireless sensor network using Kalman filter," *Ad Hoc Netw.*, vol. 11, no. 3, pp. 944–958, May 2013.
[38] A. A. Kumar, K. Ovsthus, and L. M. Kristensen, "An industrial perspective on wireless sensor networks—A survey of requirements, protocols, and challenges," *IEEE Commun. Surveys Tuts.*, vol. 16, no. 3, pp. 1391–1412, 3rd Quart., 2014.
[39] L. Zhang, Y. Wu, W. Li, H. M. Kim, S.-I. Park, P. Angueira, J. Montalban, and M. Velez, "Application of DFT-based channel estimation for accurate signal cancellation in cloud-txn multi-layer broadcasting system," in *Proc. IEEE Int. Symp. Broadband Multimedia Syst. Broadcast.*, Beijing, China, Jun. 2014, pp. 1–6.
[40] A. Mahmood, R. Exel, H. Trsek, and T. Sauter, "Clock synchronization over IEEE 802.11—A survey of methodologies and protocols," *IEEE Trans. Ind. Informat.*, vol. 13, no. 2, pp. 907–922, Apr. 2017.
[41] O. Seijo, J. A. Lopez-Fernandez, H.-P. Bernhard, and I. Val, "Enhanced timestamping method for subnanosecond time synchronization in IEEE 802.11 over WLAN standard conditions," *IEEE Trans. Ind. Informat.*, vol. 16, no. 9, pp. 5792–5805, Sep. 2020.
[42] A. Varga and R. Hornig, "An overview of the OMNeT++ simulation environment," in *Proc. 1st Int. ICST Conf. Simulation Tools Techn. Commun. Netw. Syst.*, 2008, p. 60.
[43] D. A. Wassie, I. Rodriguez, G. Berardinelli, F. M. L. Tavares, T. B. Sorensen, and P. Mogensen, "Radio propagation analysis of industrial scenarios within the context of ultra-reliable communication," in *Proc. IEEE 87th Veh. Technol. Conf. (VTC Spring)*, Porto, Portugal, Jun. 2018, pp. 1–6.

JON MONTALBAN (Member, IEEE) received the M.S. and Ph.D. degrees in telecommunications engineering from the University of the Basque Country, Spain, in 2009 and 2014, respectively. He is part of the TSR (Radiocommunications and Signal Processing) research group at the University of the Basque Country, where he is currently an Assistant Professor, involved in several research projects. He has held visiting research appointments with Communication Research Centre (CRC), Canada, and Dublin City University (DCU), Ireland. His current research interests include the area of wireless communications and signal processing for reliable industrial communications. He was a co-recipient of several best paper awards, including the Scott Helt Memorial Award to recognize the best paper published in the IEEE TRANSACTIONS ON BROADCASTING, in 2019. He has served as a reviewer for several renowned international journals and conferences in the area of wireless communications, and he currently serves as an Associate Editor for IEEE ACCESS.

ENEKO IRADIER (Graduate Student Member, IEEE) received the B.Sc. and M.Sc. degrees in telecommunications engineering from the University of the Basque Country (UPV/EHU), in 2016 and 2018, respectively, where he is currently pursuing the Ph.D. degree. Since 2015, he has been a part of the TSR Research Group, UPV/EHU. He was a Researcher with the Communications Systems Group, IK4-IKERLAN, from 2017 to 2018. During his Ph.D. studies, he did an internship with Communications Research Centre Canada, Ottawa. His current research interests include the design and development of new technologies for the physical layer of communication systems and wireless solutions for Industry 4.0. He has served as a reviewer for several renowned international journals and conferences in the area of wireless communications.

PABLO ANGUEIRA (Senior Member, IEEE) received the M.S. and Ph.D. degrees in telecommunication engineering from the University of the Basque Country, Spain, in 1997 and 2002, respectively.

He joined the Communications Engineering Department, University of the Basque Country, in 1998, where he is currently a Full Professor. He is part of the Staff of the Signal Processing and Radiocommunication Lab, where he has been involved in research on digital broadcasting (DVB-T, DRM, T-DAB, DVB-T2, DVB-NGH, and ATSC 3.0) for more than 20 years. He is coauthor of an extensive list of papers in international peer-reviewed journals, and a large number of conference presentations in digital broadcasting. He has also coauthored several contributions to the ITU-R working groups WP6 and WP3. His main research interests include the design and development of new technologies for the physical layer of communication systems in industrial wireless environments.

Dr. Angueira is a member of the IEEE BMSB International Steering Committee, an Associate Editor of the IEEE TRANSACTIONS ON BROADCASTING, and a Distinguished Lecturer of the IEEE BTS. He serves on the Administrative Committee of the IEEE BTS.

OSCAR SEIJO (Member, IEEE) received the B.Sc. and M.Sc. degrees in telecommunications engineering from the University of Oviedo, Spain, in 2015 and 2017, respectively. He is currently pursuing the Ph.D. degree with the Communications Systems Group, IKERLAN Technological Research Centre, Mondragón, Spain, in collaboration with the Signal Theory and Communications (TSC) Group, University of Oviedo, Spain. His research interests include wireless high-performance PHY and MAC design for industrial applications, time synchronization over wireless systems, and digital signal processing.

IÑAKI VAL (Senior Member, IEEE) received the B.Sc. and M.Sc. degrees from the Department of Electronics Engineering, University of Mondragon, Spain, in 1998 and 2001, respectively, and the Ph.D. degree from the Department of Signals, Systems, and Radiocommunication, Polytechnic University of Madrid, Spain, in 2011. Since 2001, he has been with the Communications Systems Group, IKERLAN, Mondragón, Spain. He has been with Fraunhofer IIS of Erlangen, Germany, as an Invited Researcher, from 2005 to 2006. He is currently a Team Leader of the Communication Systems Group. His research interests include the design and implementation of digital wireless communications systems, industrial real-time requirements, communications for distributed control systems, vehicular communications, time synchronization, wireless channel characterization, and digital signal processing. He is currently focused on industrial communication applications.